Vietnam Journal of Mechanics, Vietnam Academy of Science and Technology
DOI: https://doi.org/10.15625/0866-7136/23737

APPLICATION OF AERODYNAMIC FEATURES FROM HIGH-SPEED AIRCRAFT TO ENHANCE SAVONIUS WIND TURBINE PERFORMANCE

Phuong Nguyen Thi Thu[1,*], Minh Banh Duc[2], Anh Dinh Le[2], Tran Dang Huy[2], Yuka Iga[3], Hung The Tran[4]

[1]*Graduate School of Engineering, Tohoku University, Sendai, Japan*
[2]*School of Aerospace Engineering, VNU University of Engineering and Technology, Hanoi, Vietnam*
[3]*Institute of Fluid Science, Tohoku University, Sendai, Japan*
[4]*Le Quy Don Technical University, Hanoi, Vietnam*
E-mail: nguyen.thi.thu.phuong.t3@dc.tohoku.ac.jp

Received: 05 November 2025 / Revised: 13 December 2025 / Accepted: 26 December 2025
Published online: 11 March 2026

Abstract. As part of the global transition to sustainable energy, wind power has emerged as a promising alternative, widely adopted in Vietnam and beyond. In recent years, the Savonius wind turbine, a vertical-axis design, has offered advantages such as omnidirectional wind capture and simple structure but suffers from low aerodynamic efficiency, limiting its broader application. Inspired by the principles of aerodynamic efficiency observed in modern high-speed aircraft, such as the F-22, F-117 and TU-160, this study explores blade modifications incorporating fuselage geometry features to enhance performance. A series of computational fluid dynamics (CFD) simulations were conducted to investigate the influence of these new blade designs on the turbine's power coefficient (C_P). The results indicate that the proposed modifications can enhance C_P values by up to 13.3% compared to the conventional Savonius design, particularly at higher tip speed ratios ($\lambda > 0.8$). This improvement paves the way for the practical application of Savonius wind turbines in urban wind energy harvesting, where compact and efficient designs are essential.

Keywords: Savonius wind turbine, CFD, vertical axis wind turbine, tip speed ratio.

1. INTRODUCTION

In the current global context, renewable energy has emerged as a sustainable development trend to contribute to the energy security and environmental protection. Vietnam is regarded as a country with great potential for wind energy development due to its location in the Asian monsoon region, which features high and stable average wind speeds. Among various wind turbine technologies, the Savonius vertical axis wind turbine (VAWT) stands out for its simplicity, low cost, and adaptability to a wide range of wind conditions, making it suitable for applications in urban or rural areas.

Despite the above-mentioned advantages, the inherent limitations in efficiency still remain as the drawbacks of such systems, thus, continuous improvements in turbine design and structure are essential. Recent design initiatives have focused on optimizing or combining geometric parameters. For instance, an overlapping-blade configuration developed from the original Savonius profile was proposed and experimentally tested by Blackwell et al. (1977), resulting in a 25.5% increase in the power coefficient (C_P) at an overlap ratio of 0.1. Similarly,

a design of Bach (1931) was modified and investigated on multiple tip speed ratios (λ) by experimental methods by Roy and Saha (2015) and simulated by Kacprzak et al. (2013). The largest C_P increases to 30% at $\lambda = 0.81$. The use of multi-curved blades or elliptical blades is also investigated with the improvement of C_P up to 84% at $\lambda = 1.0$ thanks to the Bezier curve design of Zemamou et al. (2020) and 185% at $\lambda = 1.5$ in the study of Minh, Hung, et al. (2023). Though, many designs demonstrate optimal performance at low wind speeds ($\lambda < 1.0$), limiting their applicability in high-speed-wind areas. Additionally, some designs have complex geometric parameters, are difficult to produce and are only suitable for theoretical research. One emerging direction in design involves bio-inspired or aero-inspired blade geometries. Researchers have begun incorporating natural animal shapes or components from aerospace vehicles to deform blade profiles. For example, Tartuferi et al. (2015) employed airfoil SR3345 to improve performance at low speed, and SR5050 for high-speed wind. Khan et al. (2022) introduced the S1048 airfoil surface to their design, yielding a 14% performance improvement at $\lambda = 1.0$ compared to the traditional configuration. A new airfoil-shaped blade based on the FX74-CL5-140 airfoil profile, introduced by Le et al. (2024), also contributed to an increase in C_P up to 16.5% at $\lambda = 1.1$, relative to the original design. Drawing further inspiration from nature, blade profiles modeled after the shape of koi fish and sand eels (Hashem & Zhu, 2021; Ma et al., 2024) demonstrated notable performance enhancements for Savonius wind turbines.

Building upon these ideas, the present study explores the application of aerospace design elements, specifically the fuselage shapes of high-speed aircraft such as the F-22, F-117 and TU-160 to develop novel blade profiles for Savonius wind turbines. Computational Fluid Dynamics (CFD) simulations are utilized to evaluate the aerodynamic performance of these new designs in comparison to the baseline model tested by Blackwell et al. (1977).

2. AIRCRAFT-BLADE GEOMETRICAL DESIGN

In this research, the design process of the Savonius wind turbine model is carried out by drawing inspiration from the geometric principles, rather than directly transferring the operational aerodynamics, of high-speed aircraft fuselages. While it is acknowledged that these aircraft are designed for supersonic flow regimes fundamentally different from the low-speed, high-separation flow environment of a Savonius turbine, their shapes embody sophisticated solutions for flow control and pressure management. Three aircraft fuselage shapes, those of the F-22 Raptor, F-117 Nighthawk, and TU-160 Blackjack, are selected for investigations as potential blade profiles for the VAWT. These aircraft fuselages have unique geometric attributes, such as multi-curvature profiles, sharp leading edges, faceted surfaces, which are hypothesized to be repurposed for manipulating the low-speed, high-turbulence flow around a Savonius rotor. The use of these fuselage shapes aims to explore the potential of exploiting asymmetric pressure distribution effects to generate torque and improve wind energy conversion efficiency. This study also introduces a novel perspective on applying aerodynamic concepts from the aerospace domain to the design of renewable energy devices.

For benchmarking purposes, the baseline Savonius rotor is modeled according to the design proposed by Blackwell et al. (1977), consisting of two semi-cylindrical blades with a diameter of $d = 0.5$ m and a height of $H = 1$ m. The model is shown in Fig. 1 and Table 1 and for convenience, this profile is denoted as Ov01. In this configuration, the convex side of the original semi-circular blade is used as the reference baseline for constructing new profiles based on aircraft fuselage shapes, while the concave side is replaced by the natural curvature of the fuselage. The nose of the fuselage is positioned near the turbine's center, resulting in a blade thickness that gradually increases from the center to the outer edge, mimicking the natural thickness distribution of the aircraft body. The aircraft-inspired blade designs are illustrated in Fig. 2 and detailed in Table 1. F22, F117, and TU160 are labels that correspond to the three selected aircraft models.

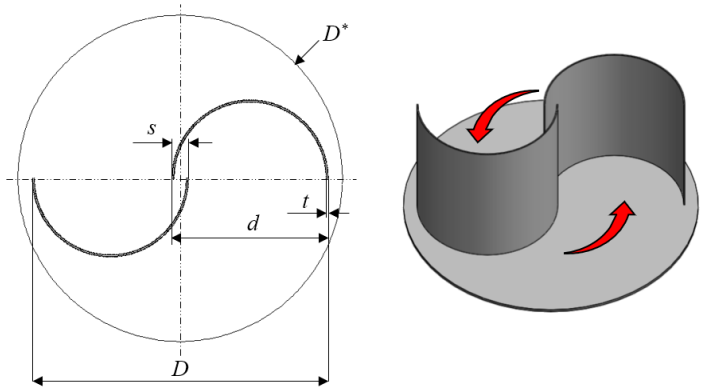

Fig. 1. Conventional configuration of Savonius wind turbine

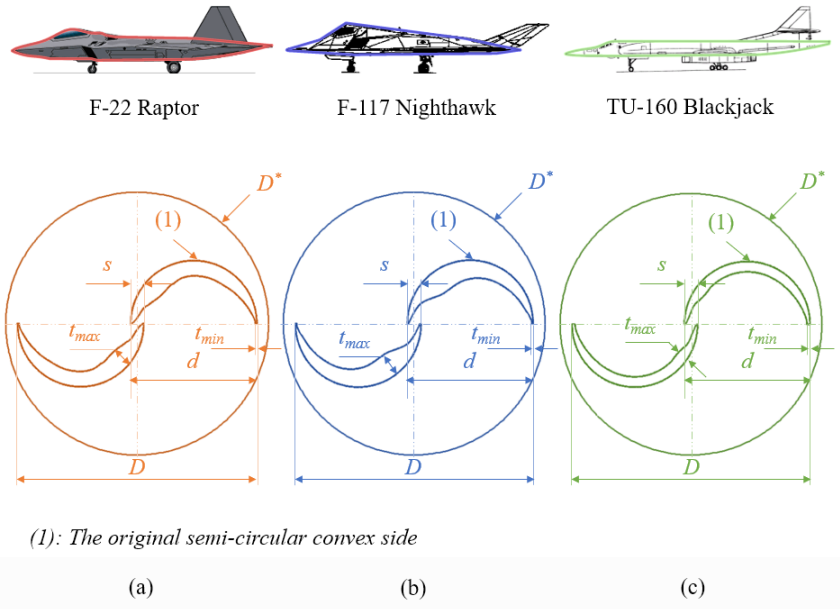

Fig. 2. Aircraft blade configuration for Savonius wind turbine based on three fuselage shapes of: (a) F-22 Raptor, (b) F-117 Nighthawk, (c) TU-160 Blackjack

Table 1. Detailed geometric parameters of four configurations

Conf.		Ov01	F22	F117	TU160
D	[m]	0.95	0.95	0.95	0.95
D^*	[m]	$1.1D$	$1.1D$	$1.1D$	$1.1D$
d	[m]	0.5	0.5	0.5	0.5
t	[m]	0.004	$t_{\min} \approx 0.004$ $t_{\max} \approx 0.078$	$t_{\min} \approx 0.004$ $t_{\max} \approx 0.091$	$t_{\min} \approx 0.004$ $t_{\max} \approx 0.044$
$e = s/d$		0.1	0.1	0.1	0.1

3. COMPUTATIONAL FLUID DYNAMICS SIMULATION

Based on the advantage of Savonius turbines having a constant cross-sectional profile along their height and the accuracy and stability of previous works (Le et al., 2024; Minh, Hung, et al.,

2023), the turbine is investigated using a two-dimensional ($2D$) numerical simulation approach with a computational domain illustrated in Fig. 3. The domain is divided into two zones: a stationary zone and a rotating zone, which are connected using an interface method. The rotating zone, which encloses the rotor, has a diameter of $D^* = 1.1D$ and is aligned along the central axis of the turbine. The inlet boundary (wind velocity inlet $U_0 = 7$ m/s) and outlet boundary (pressure outlet) are positioned along the y-axis at distances of $8D$ and $16D$, respectively, from the rotor center. Meanwhile, the side boundaries (symmetry) are placed symmetrically along the x-axis at a distance of $10D$ from the rotor center to eliminate the influence of wall effects on the flow around the rotor (Le et al., 2024).

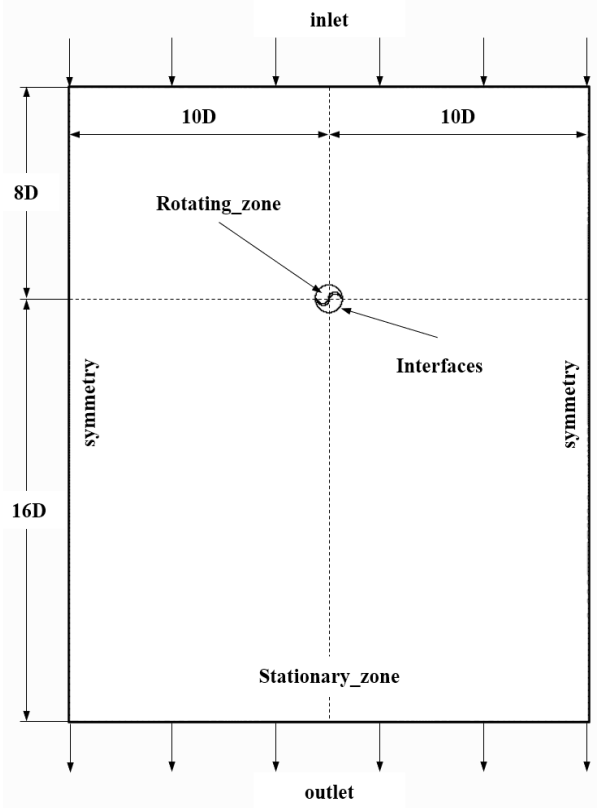

Fig. 3. Computational domain of Savonius wind turbines' simulations

For the Savonius wind turbine model, the mesh structure is designed as shown in Fig. 4, with appropriate refinement in different flow regions to ensure both high accuracy and computational efficiency. In the rotating zone, an unstructured mesh is employed, with special refinement around the blade surfaces. In contrast, the stationary zone is meshed using a structured grid, which allows for faster computation and improved accuracy in regions with more stable flow characteristics. These two zones are connected via an interface, and the transient rotor-stator interaction is resolved using the sliding mesh technique, ensuring a consistent and accurate transfer of flow data across the interface. Near the turbine blade surfaces, high-resolution boundary layer meshes are applied, with layer thickness of 10^{-5} m, to accurately capture the flow behavior within the inflation (Le et al., 2024; Minh, Hung, et al., 2023). A smooth transition is maintained between mesh layers to ensure that the y^+ value remains below 1 throughout the simulations. This is a critical requirement to accurately resolve the effects of near-wall flow dynamics.

This study employs the Unsteady Reynolds-Averaged Navier-Stokes (URANS) approach for numerical simulation, using ANSYS Fluent commercial software. The governing equations used are the two-dimensional, incompressible Navier-Stokes equations, expressed as follows

$$\frac{\partial u_i}{\partial x_i} = 0, \tag{1}$$

$$\frac{\partial \rho u_i}{\partial t} + \frac{\partial \rho u_i u_j + \delta_{ij} p}{\partial x_j} = \frac{\partial}{\partial x_j}\left(\mu + \mu_t\right)\left(\frac{\partial u_i}{\partial x_j}\right). \tag{2}$$

The GEKO turbulence model is utilized for the simulation as a newly developed turbulence model for RANS simulation with an improvement against the existing turbulence models like the SST $k-\omega$ model. The GEKO model can be expressed in terms of turbulent kinetic energy k and turbulent specific dissipation rate ω as follows (Menter et al., 2019)

$$\frac{\partial(\rho k)}{\partial t} + \frac{\partial(p u_i k)}{\partial x_i} = \frac{\partial}{\partial x_i}\left[\left(\mu + \frac{\mu_t}{\sigma_k}\right)\frac{\partial k}{\partial x_i}\right] + P_k - C_\mu \rho k \omega, \tag{3}$$

$$\frac{\partial(\rho\omega)}{\partial t} + \frac{\partial(\rho u_i \omega)}{\partial x_i} = \frac{\partial}{\partial x_i}\left[\left(\mu + \frac{\mu_t}{\sigma_\omega}\right)\frac{\partial \omega}{\partial x_i}\right] + C_{\omega 1} F_1 \frac{\omega}{k} P_k - C_{\omega 2} F_2 \rho \omega^2 + \rho F_3 CD. \tag{4}$$

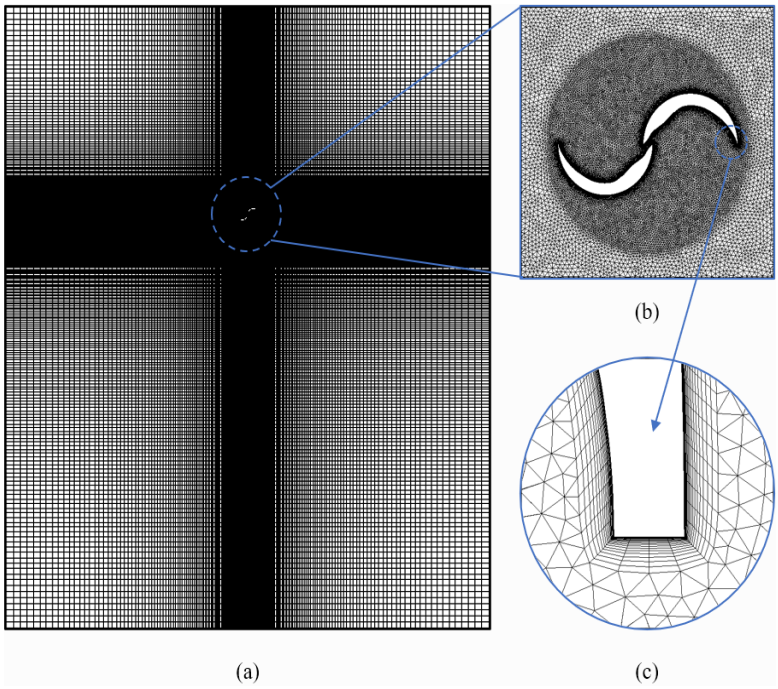

Fig. 4. Computational mesh at: (a) Whole domain, (b) Rotor region, (c) Near blades

Here, P_k is the turbulent production rate. In addition, u is the velocity component, ρ is the density of air, p is the pressure, and μ is the dynamic viscosity. The subscript t denotes the turbulent quantities. The constants $\sigma_k, \sigma_\omega, C_{\omega 1}$, and $C_{\omega 2}$ remain similar to those in the standard $k-\omega$ model (Wilcox, 1998). The functions F_1, F_2, and F_3 contain the free empirical constants (C_{sep}, C_{nw}, C_{jet}, and C_{mix}) that can be controlled for various flow scenarios (Menter et al., 2019). The optimal set of free model empirical constants, namely $C_{sep} = 1.0, C_{nw} = 2.0, C_{jet} = 1.3$, has been proven by Minh, Tran, et al. (2023) , showing that satisfactory agreement with experimental data can be obtained for either non-overlap or overlap Savonius wind turbine configuration.

For the simulation method, the pressure-based solver is employed along with the SIMPLE (Semi-Implicit Method for Pressure-Linked Equations) scheme for pressure–velocity coupling.

The second-order upwind scheme is used for discretizing the momentum and the turbulent quantities equations. For time discretization, the second-order implicit method is used in combination with the sliding mesh model, which allows accurate simulation of the rotor's transient motion. The turbine's energy conversion performance is evaluated based on key parameters, including the torque coefficient (C_T), the power coefficient (C_P), and the tip speed ratio (λ), which are calculated as follows

$$C_T = \frac{4T}{\rho H D^2 U_0^2}, \tag{5}$$

$$C_P = \frac{2P}{\rho H D U_0^3} = \lambda C_T, \tag{6}$$

$$\lambda = \frac{\omega D}{2U_0}. \tag{7}$$

In these equations, P denotes the power output of the turbine (W), while T represents the torque acting on the turbine blade (Nm). The parameter H is the height of the turbine (m), and U_0 is the freestream wind velocity (m/s). The angular velocities of the original and aircraft blade configurations are denoted as ω (rad/s). Finally, D refers to the rotor blade diameter (m). Table 2 displays various rotational speeds, denoted as ω, for each specific λ. The time step size is set to 1°/timestep for one rotation (Le et al., 2024).

Table 2. Angular velocity (ω) with respect to Tip Speed Ratio (λ)

λ	0.8	0.9	1.0	1.1	1.2	1.3	1.4
ω	11.8	13.3	14.7	16.2	17.7	19.2	20.6

4. RESULTS AND DISCUSSION

4.1. Mesh independence

Mesh independence analysis was carried out using four different meshes for each blade profile. As shown in Table 3, Mesh 2 is found to be sufficiently accurate and suitable for use in this investigation.

Table 3. Mesh independence analysis

Mesh	Elements	Torque [Nm]	Error [%]
	Ov01		
Mesh 1	107480	3.778	1.923
Mesh 2	170360	3.851	-
Mesh 3	297922	3.868	0.451
	F22		
Mesh 1	103696	3.718	2.322
Mesh 2	161066	3.804	-
Mesh 3	285734	3.795	0.230

4.2. Validation of numerical method

To verify the accuracy and applicability of the numerical method employed, Ov01 configuration was selected. The numerical simulation using the GEKO turbulent model with the optimal set of free model empirical constants, namely $C_{sep} = 1.0, C_{nw} = 2.0, C_{jet} = 1.3$ (Minh, Tran, et al., 2023). The results, shown in Fig. 5, illustrates the trend of the torque coefficient C_T obtained from the present numerical simulation (denoted as Ov01 (GEKO)) and compares it with the experimental data reported by Blackwell et al. (1977) (denoted as Ov01 (Exp.)). The small errors show that the applied numerical method is highly reliable and provides a solid foundation for the in-depth analysis in the subsequent sections of this study.

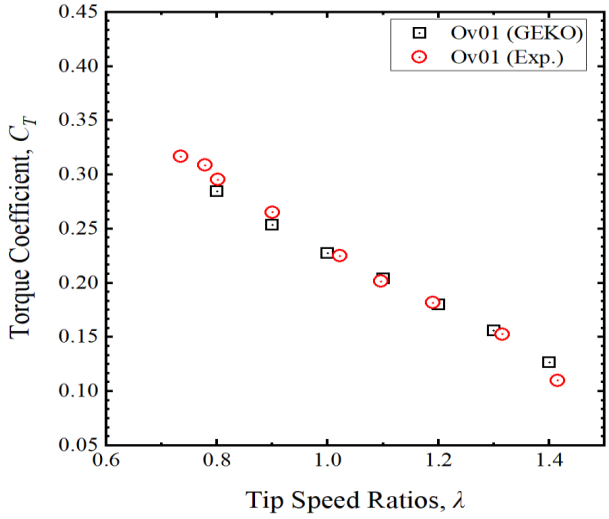

Fig. 5. Validation results for Ov01 configuration

4.3. Improvement in the averaged aerodynamic efficiency

The analysis of the data presented in Fig. 6(a) reveals a decreasing trend in the torque coefficient (C_T) as the tip speed ratio (λ) increases from 0.8 to 1.4 for all four blade profiles under investigation. At λ = 0.8, the newly proposed aircraft-inspired blades do not yet demonstrate an improvement in C_T compared to the baseline Ov01. A notable observation from this analysis is that the TU160 blade profile consistently exhibits a lower C_T than the Ov01 across the entire range of tip speed ratios, indicating that it does not yet offer superior torque performance or energy conversion potential.

Correspondingly, Fig. 6(b) illustrates the distribution of the power coefficient (C_P) for the same range of λ. All configurations show a general increasing trend in C_P as λ increases from 0.8, reaching a peak at a specific λ, and then gradually declining as λ continues to rise. This behavior reflects the turbine's ability to convert wind energy most efficiently within a certain operating range, beyond which performance diminishes due to decreasing aerodynamic drag force contributions and other dynamic effects at higher rotational speeds.

Specifically, the Ov01 configuration reaches its peak C_P at λ = 0.9, followed by a gradual decline. In contrast, the aircraft-inspired blade profiles continue to increase in C_P until reaching new peaks at λ = 1.1, effectively, extending the high-performance operating range of the Savonius wind turbine. Particularly, at this tip speed ratio, the F22 and F117 profiles exhibit improved peak C_P values compared to Ov01 by 4.12% and 7.54%, respectively. At a tip speed ratio of 1.3, these improvements rise further to 10.13% and 13.32%, respectively.

As shown in Fig. 7(a), at λ = 0.8, the torque coefficient values generated by the two newly designed aircraft-inspired blade profiles exhibit minimal difference compared to the original Ov01

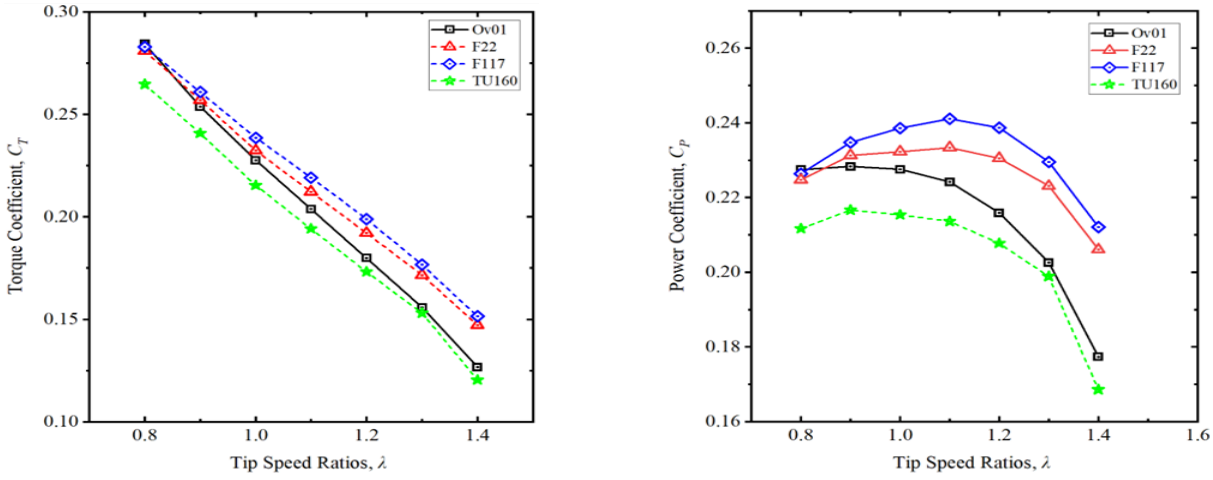

Fig. 6. Comparison of (a) Torque Coefficient (C_T), (b) Power Coefficient (C_P) among four configurations

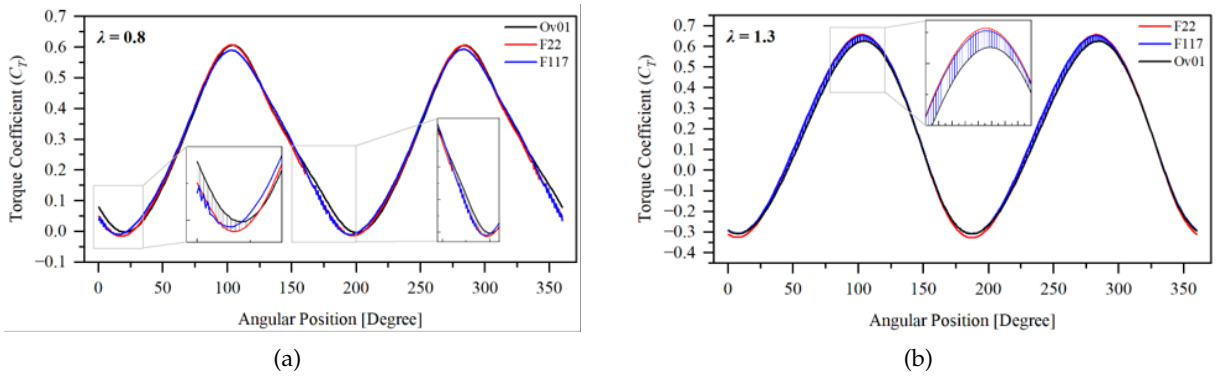

Fig. 7. Torque coefficient (C_T) in one rotation of three configurations at (a) $\lambda = 0.8$, (b) $\lambda = 1.3$

configuration across most angular positions. In fact, within the angular ranges approximately −15 degrees to 15 degrees and its symmetric counterpart from 165 degrees to 195 degrees, the Ov01 profile even produces higher torque values. This indicates that at low tip speed ratios, the new blades do not yet demonstrate a clear advantage in torque generation over the conventional profile.

However, as the turbine rotates faster, specifically at a tip speed ratio of 1.3, the F22 and F117 profiles exhibit torque coefficient distributions that are not only closely aligned with each other but also show superior performance compared to Ov01 in the angular ranges of approximately 45 degrees to 120 degrees, and symmetrically from 225 degrees to 300 degrees. As a result, the integrated torque coefficient over a full rotation is improved, reflecting a net enhancement in aerodynamic performance relative to the original blade shape.

4.4. Flow field parameters' distribution

In this section, the flow characteristics around the turbine are analyzed to evaluate the aerodynamic improvements introduced by the investigated profiles. As shown in the pressure distribution at a tip speed ratio of 0.8 (Fig. 8), the natural curvature and thickness of the aircraft-inspired profiles, F22 and F117, present certain disadvantages in capturing the incoming flow on the concave side of the advancing blade (black). This results in a smaller high-pressure region

on this surface compared to the Ov01 profile, thereby reducing the pressure difference between the two sides of the blade. Consequently, lower positive torque is generated, leading to poorer aerodynamic performance. In addition, the velocity contours reveal that the narrow overlap gap, shaped by the geometry of the aircraft-inspired blades, forms a flow channel that accelerates the flow passing through it. This high-speed jet then remains attached to the concave surface of the returning blade (blue), creating a low-pressure region that opposes the turbine's rotation. These combined effects explain why the F22 and F117 configurations fail to improve aerodynamic efficiency at a tip speed ratio of 0.8.

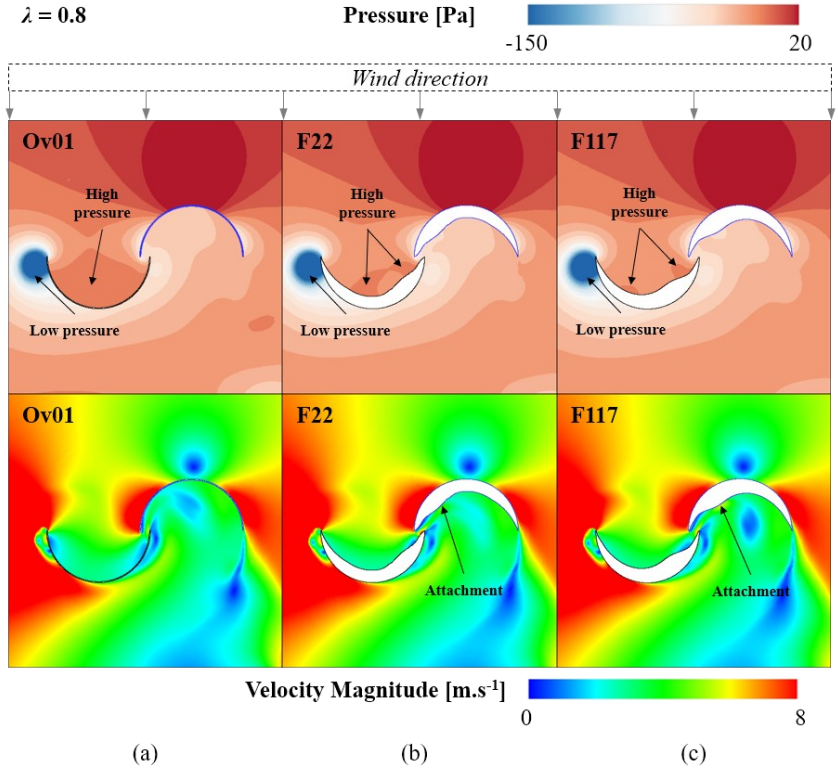

Fig. 8. Pressure and velocity distribution at λ = 0.8 and angular position of 0 degree for (a) Ov01 conf., (b) F22 conf., (c) F117 conf.

To further investigate the performance improvements brought by the F22 and F117 blade profiles, the velocity distribution around the rotor at a tip speed ratio of 1.3 was analyzed. The angular positions of 60 degrees and 90 degrees are selected due to the significant differences in torque generation observed among profiles at these positions, as shown in Fig. 7(b). At this operating condition, it is observed that the accelerated flow through the overlap gap effectively eliminates the vortex typically found within the gap in the Ov01 configuration. This high-speed flow remains attached to the surface of the advancing blade (black), helping to maintain a stable pressure distribution on its concave side. In contrast, in the Ov01 profile, the lower-velocity flow passing through the overlap region separates from the concave surface of the advancing blade, leading to a local pressure drop. This flow phenomenon induces torque, which contributes to a reduction in aerodynamic performance. Therefore, at a tip speed ratio of 1.3, the improved flow behavior observed in the F22 and F117 configurations results in a clear enhancement in turbine efficiency compared to the original design.

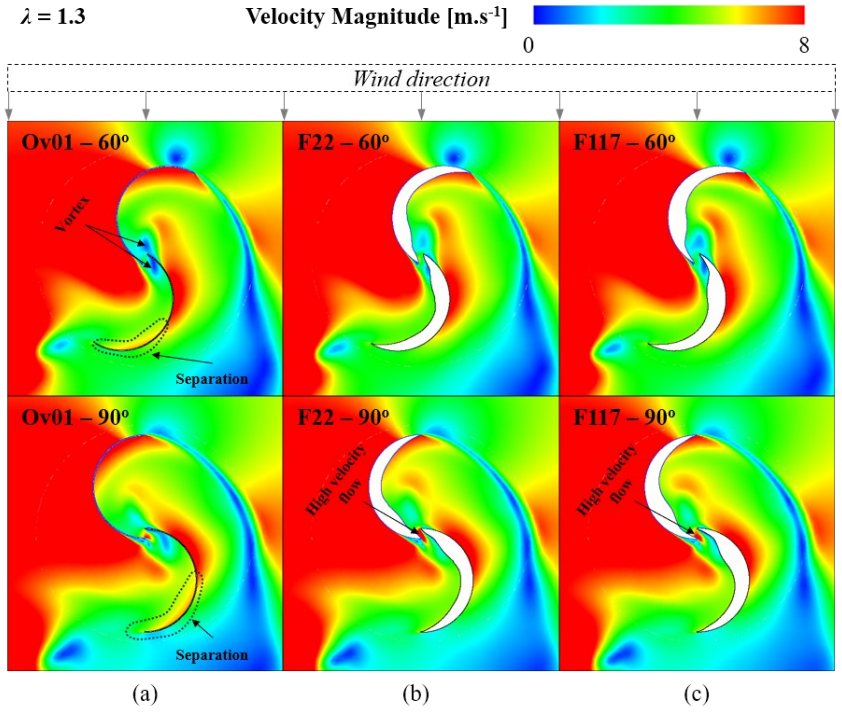

Fig. 9. Velocity distribution at $\lambda = 1.3$ and angular positions of 60 degrees and 90 degrees for (a) Ov01 conf., (b) F22 conf., (c) F117 conf.

5. CONCLUSION

This research studied a novel approach to enhance the aerodynamic efficiency of Savonius vertical axis wind turbines by drawing inspiration from the fuselage shapes of high-speed aircraft (F22, F117, and TU160). Through a series of computational fluid dynamics (CFD) simulations, the impact of these modified blades on the turbine's power coefficient (C_P) was evaluated. The results show that the strategic flow guiding and separation management can improve C_P by up to 13.3% compared to the conventional Savonius rotor, especially at higher tip speed ratios ($\lambda > 0.8$). Crucially, the study also revealed that not all complex shapes are beneficial, as demonstrated by the underperformance of the TU160 profile, highlighting that the transfer of aerodynamic concepts must be critically evaluated for the flow regime of Savonius wind turbines. Rather than proposing specific shapes for direct practical application, this work provides fundamental design insights and a proof-of-concept that leveraging advanced aerodynamic principles from aerospace can be a fruitful direction for Savonius turbine optimization. Future work will focus on extracting and isolating the key geometric parameters to develop generalized and practical design guidelines for next-generation urban wind energy harvesters.

DECLARATION OF COMPETING INTEREST

The authors declare that they have no known competing financial interests or personal relationships that could have appeared to influence the work reported in this paper.

CREDIT AUTHOR STATEMENT

Phuong Nguyen Thi Thu: *Formal analysis, Software, Data Curation, Validation, Writing – original draft*. Minh Banh Duc: *Investigation, Validation, Writing – review & editing*. Anh Dinh Le: *Supervision, Methodology, Conceptualization, Writing – review & editing*. Tran Dang Huy:

Investigation, Validation, Writing – review & editing. Yuka Iga: *Supervision, Methodology, Writing – review & editing*. Hung The Tran: *Software, Resources, Validation, Writing – review & editing*.

ACKNOWLEDGEMENT

This research is funded by Vietnam National Foundation for Science and Technology Development (NAFOSTED) under grant number 107.03-2023.05.

REFERENCES

Bach, G. (1931). Untersuchungen über savonius-rotoren und verwandte strömungsmaschinen. *Forschung auf dem Gebiete des Ingenieurwesens*, *2*(6), 218–231. https://doi.org/10.1007/bf02579117

Blackwell, B. F., Feltz, L. V., & Sheldahl, R. E. (1977). *Wind tunnel performance data for two- and three-bucket Savonius rotors*. Sandia Laboratories, Springfield, VA, USA.

Hashem, I., & Zhu, B. (2021). Metamodeling-based parametric optimization of a bio-inspired Savonius-type hydrokinetic turbine. *Renewable Energy*, *180*, 560–576. https://doi.org/10.1016/j.renene.2021.08.087

Kacprzak, K., Liskiewicz, G., & Sobczak, K. (2013). Numerical investigation of conventional and modified Savonius wind turbines. *Renewable Energy*, *60*, 578–585. https://doi.org/10.1016/j.renene.2013.06.009

Khan, Z. U., Ali, Z., & Uddin, E. (2022). Performance enhancement of vertical axis hydrokinetic turbine using novel blade profile. *Renewable Energy*, *188*, 801–818. https://doi.org/10.1016/j.renene.2022.02.050

Le, A. D., Thu, P. N. T., Doan, V. H., Tran, H. T., Banh, M. D., & Truong, V.-T. (2024). Enhancement of aerodynamic performance of Savonius wind turbine with airfoil-shaped blade for the urban application. *Energy Conversion and Management*, *310*, 118469. https://doi.org/10.1016/j.enconman.2024.118469

Ma, C., Wang, G., Wang, D., Peng, X., Yang, Y., Liu, X., Yang, C., & Chen, J. (2024). Optimization design and performance analysis of a bio-inspired fish-tail vertical axis wind rotor. *Energy Conversion and Management*, *300*, 117901. https://doi.org/10.1016/j.enconman.2023.117901

Menter, F., Lechner, R., & Matyushenko, A. (2019). *Best practice: Generalized k-ω two-equation turbulence model in ANSYS CFD (GEKO)*. ANSYS Germany GmbH.

Minh, B. D., Hung, T. T., Duc, N. D., Trinh, C. D., & Anh, D. L. (2023). Performance enhancement of Savonius wind turbine by multicurve blade shape. *Energy Sources, Part A: Recovery, Utilization, and Environmental Effects*, *45*(1), 1624–1642. https://doi.org/10.1080/15567036.2023.2180114

Minh, B. D., Tran, T. H., Pham Van, K., & Le, A. D. (2023). Predicting aerodynamic performance of Savonius wind turbine: An application of generalized *k-ω* turbulence model. *Ocean Engineering*, *286*, 115690. https://doi.org/10.1016/j.oceaneng.2023.115690

Roy, S., & Saha, U. K. (2015). Wind tunnel experiments of a newly developed two-bladed Savonius-style wind turbine. *Applied Energy*, *137*, 117–125. https://doi.org/10.1016/j.apenergy.2014.10.022

Tartuferi, M., D'Alessandro, V., Montelpare, S., & Ricci, R. (2015). Enhancement of Savonius wind rotor aerodynamic performance: A computational study of new blade shapes and curtain systems. *Energy*, *79*, 371–384. https://doi.org/10.1016/j.energy.2014.11.023

Wilcox, D. C. (1998). *Turbulence modeling for CFD* (Vol. 2). DCW Industries.

Zemamou, M., Toumi, A., Mrigua, K., Lahlou, Y., & Aggour, M. (2020). A novel blade design for Savonius wind turbine based on polynomial Bezier curves for aerodynamic performance enhancement. *International Journal of Green Energy*, *17*(11), 652–665. https://doi.org/10.1080/15435075.2020.1779077